Simulations of beam emittance growth from the collective relaxation of space-charge nonuniformities

Steven M. Lund[a],*, David P. Grote[a], Ronald C. Davidson[b]

[a]Lawrence Livermore National Laboratory, Livermore, CA 94550, USA
[b]Princeton Plasma Physics Laboratory, Princeton, NJ 08543, USA

Available online 26 February 2005

Abstract

Beams injected into a linear focusing channel typically have some degree of space-charge nonuniformity. For unbunched beams with high space-charge intensity propagating in linear focusing channels, Debye screening of the self-field interaction between particles tends to make the transverse density profile flat. An injected particle distribution with a large systematic charge nonuniformity will generally be far from an equilibrium of the focusing channel and the initial condition will launch a broad spectrum of collective modes. These modes can phase-mix and experience nonlinear interactions which result in an effective relaxation to a more thermal-equilibrium-like distribution characterized by a uniform density profile. This relaxation transfers self-field energy from the initial space-charge nonuniformity to the local particle temperature, thereby increasing beam phase space area (emittance growth). Here we employ two-dimensional electrostatic particle-in-cell (PIC) simulations to investigate the effects of initial transverse space-charge nonuniformities on the statistical emittance growth of beams with high space-charge intensity propagating in a continuous focusing channel. Results are compared to theoretical bounds of emittance growth developed in previous studies. Consistent with earlier theory, it is found that a high degree of initial distribution nonuniformity can be tolerated with only modest emittance growth and that beam control can be maintained. The simulations also provide information not addressed by the theory on the rate of relaxation and characteristic levels of fluctuations in the relaxed states. This research suggests that a surprising degree of initial space-charge nonuniformity can be tolerated in practical intense beam experiments.

1. Introduction

Experiments with high-current, heavy-ion injectors have observed large space-charge

---
*Corresponding author.
  E-mail address: SMLund@llnl.gov (S.M. Lund).

nonuniformities in the beam emerging from the source [1]. Sharp density peaks on the radial edge of beam have been measured. Non-ideal forces from aberrations of the applied focusing system and other sources can also result in transverse density profiles that have strongly nonuniform charge density. In ideal linear focusing systems of space-charge-dominated beams, the transverse space-charge distribution of an ion beam tends to be nearly uniform within an elliptical envelope boundary. This produces nearly linear transverse self-field forces within the beam that preserve the beam phase space area (emittance). Theoretical work has described collective modes internal to the core of an intense continuously focused beam [2]. This work suggests that sharp initial density perturbations typically decompose into a broad spectrum of collective modes. For moderate space-charge strength (warm beam), the oscillation frequencies of the individual linear modes vary strongly thereby leading to rapid phase mixing. Also, the modes nonlinearly interact and Landau damp. These processes tend to disperse the initial perturbation structure and result in a more uniform, relaxed density profile with residual fluctuations.

The spatially averaged particle temperature of a heavy ion beam emerging from an injector is typically measured as several times what one would infer from the source thermal temperature ($\sim 0.1\,\mathrm{eV}$), and subsequent beam envelope compressions result in a beam with $\bar{T}_x \sim 20\,\mathrm{eV}$, where $\bar{T}_x \sim [\varepsilon_x^2/(2R^2)]E_\mathrm{b}$. On the other hand, the radial change in potential energy from the beam center to the outer radial edge is $q\Delta\phi \sim 2.25\,\mathrm{keV}$ for a beam with line-charge density $\lambda \sim 0.25\,\mu$ C/m [$\Delta\phi \sim \lambda/(4\pi\varepsilon_0)$]. If even a small fraction of such space-charge energy is "thermalized" during collective relaxation, large temperature and emittance increases can result. There have also been concerns that even if the perturbations launched do not relax that they could lead to a loss of beam control or excessive halo production resulting from oscillating nonlinear self-field forces internal to the beam. Theoretical work based on simple charge and energy conservation arguments, augmented by the rms envelope equations, show that the amount of free energy carried by the charge

nonuniformities that can be converted to emittance growth is in fact relatively small [3,4]. This work extends earlier theories by Reiser and others [5–7] and demonstrates that even large initial density nonuniformities with strong beam space-charge strength only produce modest growth in beam emittance.

Earlier theories did not address details of relaxation processes and assumed that an initial nonuniform density beam would relax to a uniform profile via collective processes. The theory assumed complete relaxation to establish an upper bound of emittance growth. Here we employ the two-dimensional transverse slice module of the WARP electrostatic particle-in-cell (PIC) code to simulate the relaxation process [8]. Results show that collective effects tend to cause an initial beam with strongly nonuniform density to relax to a state that is equilibrium-like with a more uniform, smooth density profile, and low-order residual oscillations. The simulations also provide information not addressed by the theory such as the rapidity of the effective relaxation processes and the characteristic fluctuation levels about the relaxed state since there is not in general full relaxation. This process is simulated for a wide variety of initial beam space-charge strengths and distribution profiles.

2. Description of the WARP PIC simulations

Simulation parameters are based on an unbunched coasting ($\beta_\mathrm{b} = \mathrm{const}$) intense K^+ ($m = 39.1\,\mathrm{amu}$) ion beam with particle kinetic energy $E_\mathrm{b} = (\gamma_\mathrm{b} - 1)mc^2 = 1.0\,\mathrm{MeV}$ and zero spread in axial momentum. Applied focusing is provided by a linear continuous focusing field corresponding to a radial electric field of a uniform, noninteracting background of partially neutralizing charges. The field is set to approximately correspond to typical beam parameters in periodic focusing lattices for heavy ion fusion by requiring that a single particle oscillating in the field has a phase advance $\sigma_0 = 80°$ when measured through an axial propagation distance (lattice period) of $L_p = 0.5\,\mathrm{m}$. The initial beam has rms edge emittance $\varepsilon_x = \varepsilon_y = 50\,\mathrm{mm\text{-}mrad}$ and the

injected beam current I is adjusted to obtain specified values of the single-particle phase advance in the presence of space-charge (σ). The value of σ is calculated for an rms-equivalent KV-matched beam with uniform space charge [5].

Transverse statistical averages over an axial slice of the particle distribution f are denoted by $\langle \cdots \rangle_\perp$. Primes denote derivatives with respect to the axial coordinate s. Along the x-axis, the statistical beam edge radius and rms edge emittance are defined as

$$r_x = 2\sqrt{\langle x^2 \rangle_\perp} \tag{1}$$

and

$$\varepsilon_x = 4[\langle x^2 \rangle_\perp \langle x'^2 \rangle_\perp - \langle xx' \rangle_\perp]^{1/2}. \tag{2}$$

Analogous expressions apply along the y-axis.

A flexible distribution loading module of the WARP code is employed to load an initial ($s = 0$) axisymmetric distribution of macro-particles $f(x, y, x', y')$ consistent with independently-specified, gridded radial profiles in density, radial flow velocity, and Gaussian-distributed local velocity spread. The initial radial density profile $n = \int d^2x'_\perp f_\perp$ is given by [3,4]

$$n(r) = \begin{cases} \hat{n}\left[1 + \frac{1-h}{h}\left(\frac{r}{r_b}\right)^p\right], & 0 \leqslant r \leqslant r_b, \\ 0, & r_b < r \leqslant r_p. \end{cases} \tag{3}$$

Here, $r = \sqrt{x^2 + y^2}$ is the transverse radial co-ordinate, $r = r_b$ is the physical edge-radius of the beam, $\hat{n} = n(r = 0)$ is the on-axis ($r = 0$) beam density, and h and p ($p \geqslant 0$) are "hollowing" and "steepening index" parameters associated with the radial density nonuniformity. The hollowing parameter $h = n(r = r_b)/n(r = 0)$ corresponds to the ratio of beam density at the outer radial edge of the beam [$n(r = r_b)$] to the density at the beam center [$n(r = 0) = \hat{n}$]. For $0 \leqslant h < 1$, the density is hollowed on-axis, and for $0 \leqslant 1/h < 1$, the density is peaked on-axis. The limit $h \to 1$ corresponds to a uniform density beam regardless of the value of p. On the other hand, the limits $h \to 0$ and $1/h \to 0$ correspond to hollowed and peaked beams with the density approaching zero on-axis and at the beam edge ($r = r_b$), respectively. For large steepening index $p \gg 1$, the density gradient will be significant only near the radial edge of the beam ($r \simeq r_b$). The initial radial flow velocity

$\int d^2x'_\perp (x'\mathbf{e}_x + y'\mathbf{e}_y)f_\perp$ is taken to be zero. A function with the same form as Eq. (3) is used to set the initial radial temperature profiles $T_x(r) = (\gamma_b m\beta_b^2 c^2 \int d^2x'_\perp x'^2 f_\perp)/(\int d^2x'_\perp f_\perp)$ with $T_y(r) = T_x(r)$ defined analogously. These temperature profiles set the Gaussian-distributed spread in x' and y' as a function of r. Overall scales are set consistently from the beam edge radius r_b and the statistical rms emittances with $\varepsilon_x = \varepsilon_y$.

The line-charge density (λ) and rms edge-radius ($R = r_x = r_y$) of the axisymmetric initial beam are related to the density profile parameters in Eq. (3) by [3,4]

$$\lambda = \int d^2x_\perp \, n = \pi q \hat{n} r_b^2 \left[\frac{(ph+2)}{(p+2)h}\right],$$

$$R = 2\langle x^2 \rangle_\perp^{1/2} = \sqrt{\frac{(p+2)(ph+4)}{(p+4)(ph+2)}} r_b. \tag{4}$$

Using these expressions, the beam density profile $n(r)$ given by Eq. (3) is plotted in Fig. 1 as $n(r)/[\lambda/(q\pi R^2)]$ vs. r/R to illustrate changes in the radial beam density profile with several values of steepening index p at fixed charge ($\lambda = $ const) and rms beam size ($R = $ const). In Fig. 1 hollowed beams are plotted along with the uniform density case ($h = 1$) for reference. Analogous plots hold for the initial temperature profile. Appropriate choices of h and p allow a wide range of initial hollowed and peaked profiles to be modeled. For the special case of $h = 1$ for both the density and temperature
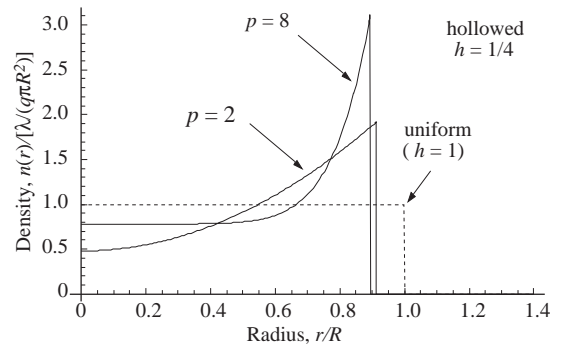

Fig. 1. Scaled density profile $n(r)/[\lambda/(\pi q R^2)]$ from Eq. (3) plotted vs. r/R with fixed λ and R. Hollowed ($h = \frac{1}{4}$) profiles are shown for $p = 2$ and $p = 8$. The rms equivalent uniform ($h = 1$) profile is shown with a dashed curve.

profiles, this initial distribution reduces to the frequently-used semi-Gaussian with a spatially uniform distribution of particle coordinates x and y and incoherent Gaussian-distributed velocity spreads in x' and y' within a round beam envelope ($r_x = r_y$). The semi-Gaussian distribution provides a reasonable approximation to a relaxed, strongly space-charge dominated beam emerging from a long transport channel where the density is expected to be nearly uniform and the beam-edge sharp [9].

For continuous focusing channels, infinite families of equilibrium distributions can be constructed by specifying any function $f(H_\perp)$ with $f \geqslant 0$ where $H_\perp$ is the transverse particle Hamiltonian [5,6]. On the other hand, for the hollowed and peaked distributions specified above, the initial beam is far from equilibrium form. Particles will generally be strongly out of local radial force balance and the beam will quickly evolve away from the initial condition. For a nonequilibrium distribution, the rms edge emittance in Eq. (2) is conserved only if all forces acting on the particles are linear [7,10]. Variation in ε_x arising from the evolution in the charge density profile can provide a sensitive measure of undesired nonlinear self-field forces acting on the beam.

Numerical parameters of the simulations are set to resolve nonlinear space-charge fields and a sharp beam edge. Spatial grids are uniform with typical transverse grid increments $dx = dy$ chosen for 50–200 grids across the initial edge radius of the beam (i.e., from $r = 0$ to $r = r_b$). The beam is contained by a round, perfectly conducting cylindrical pipe of sufficient radius to prevent particle losses. To limit statistical noise in the smoothed-beam self-field interactions and better represent ideal Vlasov evolution, we employ 100–1000 particles per grid cell in the injected beam. Particles are leap-frog-advanced with 450 steps per undepressed betatron period to resolve rapid mode phase advances and beam advances of up to 20 undepressed betatron periods are taken. Gridded data is plotted without averaging over radial zones of the axisymmetric beam to illustrate the numerical noise and to help guide non-axisymmetry periodic

focusing beam simulations not shown in this paper.

3. Theoretical results

In general, a strongly nonequilibrium beam will launch a broad spectrum of waves that can be thought of as mode-like perturbations evolving on an underlying pseudo-equilibrium beam with a smooth density profile. The pseudo-equilibrium density profile is expected to be nearly flat for beams with high space-charge intensity. If the pseudo-equilibrium is stable, one expects the perturbations to phase-mix, Landau damp, and nonlinearly interact to cause the density profile to relax to a more uniform profile with persistent, residual fluctuations. If the fluctuations are neglected, system conservation constraints can be employed to connect the initial beam distribution to a final, fully-relaxed pseudo-equilibrium profile with uniform density. These constraints can be employed to estimate emittance growth driven by the free energy conversion of the waves.

For a continuous focusing channel, the initial axisymmetric beam distribution with a nonuniform ($h \neq 1$) density profile given by Eq. (3) and an *arbitrary* distribution in $\mathbf{x}'$ can be connected to a final, relaxed axisymmetric beam distribution with uniform density ($h = 1$) by the charge and energy conservation constraints maintained by the Vlasov evolution. Assuming that both the initial (subscript i) and final (subscript f) distributions are rms-matched, a theoretical analysis of the conservation constraints [3,4] shows that

$$\frac{(R_f/R_i)^2 - 1}{1 - (\sigma_i/\sigma_0)^2} + \frac{p(1-h)[4 + p + (3+p)h]}{(p+2)(p+4)(2+ph)^2}$$
$$- \ln\left[\sqrt{\frac{(p+2)(ph+4)}{(p+4)(ph+2)}} \frac{R_f}{R_i}\right] = 0. \quad (5)$$

Here, h and p are the hollowing factor and steepening index of the initial density profile, and σ_i/σ_0 is the initial space-charge intensity. This nonlinear constraint equation can be solved numerically for fixed h, p, and σ_i/σ_0 to determine the ratio of final to initial rms radius of the beam

(R_f/R_i) which can then be used to calculate the ratio of the final to initial beam emittance from [3,4]

$$\frac{\varepsilon_{xf}}{\varepsilon_{xi}} = \frac{R_f}{R_i} \sqrt{\frac{(R_f/R_i)^2 - [1 - (\sigma_i/\sigma_0)^2]}{(\sigma_i/\sigma_0)^2}}. \qquad (6)$$

Eqs. (5) and (6) were solved numerically in Refs. [3,4] to parametrically analyze the emittance growth $(\varepsilon_{xf}/\varepsilon_{xi})$ from the relaxation of an initial rms matched beam $(R_i' = 0 = R_i'')$ with nonuniform hollowed and peaked density profiles to a final, uniform, matched profile. Surprisingly modest emittance growth factors (factor of 2 and less) were found even for strongly hollowed $(0.1 > h > 1)$ beams for intense space-charge parameters with $\sigma_i/\sigma_0 \sim 0.1$ and greater. As expected, much less growth was observed for beams with initially peaked density profiles $(h > 1)$ because such profiles are closer to uniform and contain less free field energy that can be converted into emittance growth.

It can be shown that the field energy of a uniform density beam is a global minimum when compared to all other density profiles with the same line-charge and rms radius [3,4]. Therefore a distribution relaxation that evolves a nonuniform density beam to a uniform density beam has maximal free energy to drive emittance growth relative to all other possible relaxations. It follows that the emittance growths calculated from the formulation above should provide an upper bound for continuous focusing since real evolutions will not, in general, achieve full relaxation. Although the above analysis assumes that the beam relaxes to a uniform density core, further analysis shows that only small reductions in the predicted upper-bound emittance growths if the initial beam relaxes to a diffuse thermal equilibrium density profile rather than a uniform density beam [9,4]. This result holds result over the full range of space charge strength $0 \leqslant \sigma_i/\sigma_0 \leqslant 1$. For $\sigma_i/\sigma_0 \to 0$ the thermal equilibrium profile will have uniform density, and for $\sigma_i/\sigma_0 \to 1$ it will be a bell-shaped Gaussian profile.

4. Simulation results

The theory outlined in Section 3 has been checked with PIC simulations described in Section 2.

Simulations are carried out for a range of space-charge strength and a wide variety of initial density and temperature profiles. The space-charge strength is specified by the value of σ_i/σ_0 for the initial rms-equivalent beam with uniform density. Initial density profiles are hollowed $(h < 1)$ in radius and initial temperature profiles are flat $(h = 1)$, hollowed $(h < 1)$, or peaked $(1/h < 1)$.

Results from the simulations are shown in Figs. 2 and 3 and are summarized in Table 1. In Fig. 2, a typical history of rms emittance growth $(\varepsilon_x/\varepsilon_{xi})$ is plotted for an initial beam with $\sigma_i/\sigma_0 = 0.2$ and a strongly hollowed density profile $(h = \frac{1}{4}, p = 8)$ and a parabolic temperature profile $(h = \infty, p = 2)$. The emittance undergoes a rapid evolution during the initial transient phase of the wave and then settles down to a persistent fluctuation with several lower-order frequency components. For higher values of σ_i/σ_0 the persistent oscillation also appears to slowly damp. Moreover, the average value of the fluctuating emittance is only associated with relatively modest total emittance growth from the initial profile despite the high space-charge intensity and the strongly hollowed initial density profile. Substantial "ringing" back
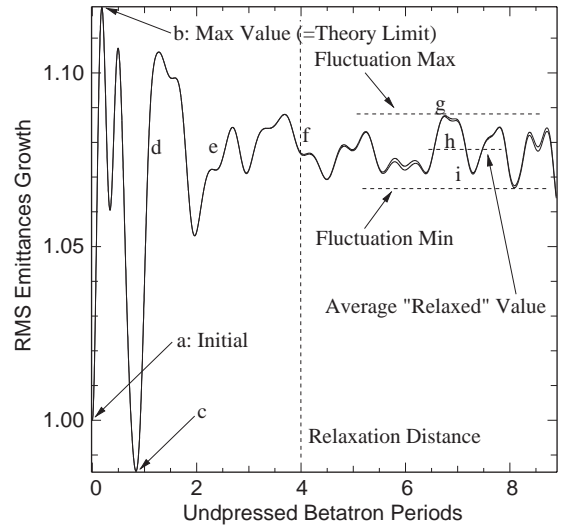

Fig. 2. Emittance growth $\varepsilon_x/\varepsilon_{xi} = \varepsilon_y/\varepsilon_{yi}$ vs. undepressed betatron oscillations $(s/[\sigma_0/(2\pi L_p)])$ for a continuous focused beam with a strongly hollowed $(h = \frac{1}{4}, p = 8)$ initial density profile and a parabolic $(h = \infty, p = 2)$ initial temperature profile.
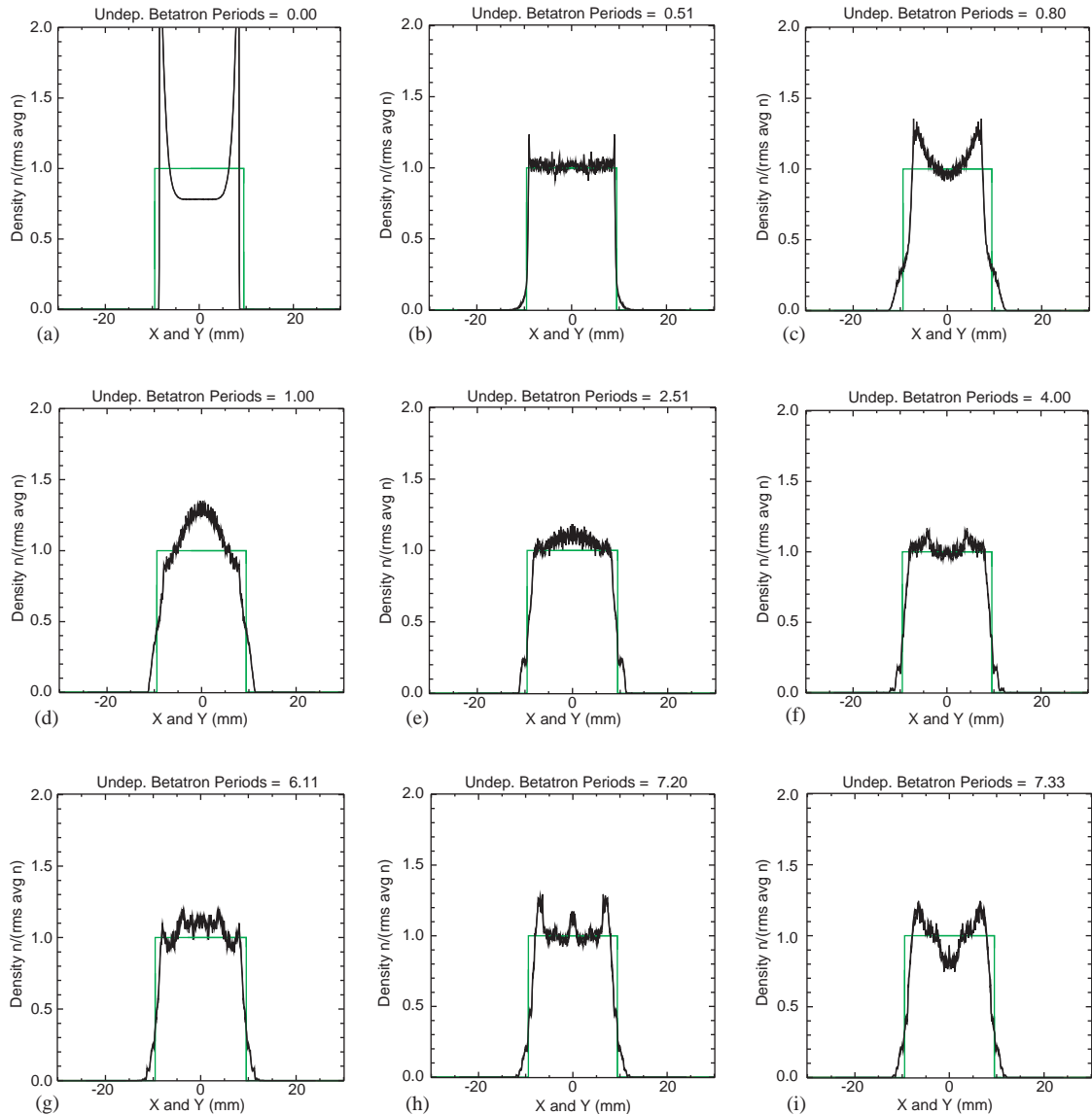
Fig. 3. Density profile snapshots of an evolving continuously focused beam corresponding to the emittance evolution in Fig. 2. The rms-equivalent uniform density beam is superimposed.

of the initial density perturbation is not observed over the length of the simulations. Beam density profile snapshots along the x-axis are plotted in Fig. 3 at the points labeled a–i in Fig. 2. Note that the 4 to 1 hollowing ($h = \frac{1}{4}$) of the initial density profile has been cut off to display all plots on the same scale and better observe fluctuations in the relaxed state. Also indicated in Fig. 2 are the

values of the "relaxed" emittance growth and the fluctuation level as well as the approximate distance of beam propagation measured in undepressed betatron periods that is needed for the emittance to settle down to a persistent fluctuation. The emittance growth factor predicted by the theory in Section 3 assuming full relaxation to a uniform density profile is also indicated in Fig. 2.

Table 1
Results of collective evolution for beams with hollowed initial density profiles in a continuous focusing channel. Blank entries are repeated from the previous line above. Simulated emittance growth estimates correspond to the average value in the relaxed state, and in brackets (peak growth value, range of oscillations in the relaxed state: min–max)

Initial beam					Relaxed and transient beam		
σ_i/σ_0	Density		Temperature		Emittance growth		Undep. betatron periods to relax
	h	p	h	p	Theory	Simulation	
0.1	0.25	4	1	arb.	1.57	1.42 (1.57, 1.31–1.52)	3.5
			∞	2		1.45 (1.57, 1.38–1.52)	3.0
			0.5			1.41 (1.57, 1.30–1.52)	3.0
	0.25	8	1	arb.	1.43	1.33 (1.43, 1.28–1.38)	3.5
			∞	2		1.35 (1.43, 1.30–1.40)	4.5
			0.5			1.32 (1.43, 1.26–1.38)	4.0
0.20	0.25	4	1	arb.	1.17	1.11 (1.16, 1.09–1.13)	4.5
			∞	2		1.12 (1.16, 1.10–1.13)	3.0
			0.5			1.11 (1.16, 1.09–1.13)	4.0
	0.25	8	1	arb.	1.12	1.08 (1.12, 1.06–1.09)	5.5
			∞	2		1.08 (1.12, 1.07–1.09)	4.0
			0.5			1.08 (1.12, 1.06–1.09)	4.5

Note that emittance growth factors measured at the peak value of the emittance oscillations correspond to more uniform radial density profiles with corresponding growthfactors that closely approach the theoretical bound.

Properties of the evolution in Figs. 2 and 3 are summarized in Table 1. Data for other simulations with differing space-charge strengths (σ_i/σ_0 values) and initial distributions (h and p values for the radial density and temperature profiles) are also presented in Table 1. We find that the different initial beam parameters and space-charge strengths result in analogous evolutions. Results are consistent with a broad spectrum of internal collective modes being launched inside the beam that then phase-mix and nonlinearly interact to cause the beam to relax to an state with increased emittance. Note that flat ($h = 1$), peaked ($h \to \infty$), and hollowed ($h = 0.5$) radial temperature profiles are simulated for the same space-charge strength and radial density profile. In general, negligible rms envelope mismatch observed during the evolution of the internal collective waves and the associated flattening of the density profile. Generation of halo particles outside the main core of

the beam appears to be minimal and higher-order (i.e., remaining close to the rms beam edge and not driven by envelope mismatch).

Comparing data in Table 1 from simulations of emittance growth for beams with the same space charge strength and density profile with differing temperature profiles, it is evident that the emittance growth depends only weakly on the structure of the initial temperature profile. In theory, there should be no dependence on the initial temperature profile if there is complete relaxation. However, the varying initial temperature profiles launch radically different wave spectra that can result in evolutions with different levels of fluctuation about the "relaxed" states. This effect probably accounts for most of the differences in the emittance growth between initial states with the same density profile observed. Also, the differing initial conditions can require different propagation distances to settle down due to the initial states projecting on different mode spectra. In all cases, the residual fluctuations appear to project primarily on low-order collective modes internal to the core of the beam. Increased space-charge strength generally results in less damping of

the initial perturbations due to decreased frequency spread in the mode spectrum. It is also observed that the propagation distance and the final level of fluctuations can vary with the amplitude of the initial perturbations indicating the presence of nonlinear effects (not pure phase-mixing). Propagation distances to the relaxed state listed in Table 1 represent only rough estimates that are measured as the distance of propagation needed for the emittance oscillations to remain bounded by a persistent fluctuation. Obtaining accurate relaxation distances is difficult because the mode fluctuations appear to experience slow Landau damping that becomes stronger for higher values of σ_i/σ_0. The "relaxed" value of the emittance is calculated from the average value (taken over the fluctuations) of the emittance oscillation about the relaxed state. Similar results to the density profile evolution in Fig. 3 are observed when the radial temperature profile is calculated from the particle distribution. The radial temperature profile in the relaxed state is observed to be more uniform with persistent lower-order fluctuations.

It should be emphasised that real accelerator systems will have small nonlinear applied fields with *both* periodic (systematic) and aperiodic (construction error) terms that will further inhibit wave packets from ever achieving phase coherence to allow initial perturbations to substantially ring back—even in long lattices. In addition, other small non-ideal effects in real machines such as species contamination, scattering, etc., will likely further suppress significant ringing. As a practical matter, the influence of nonlinear applied fields and other non-ideal effects on the evolution of a broad spectrum of waves is extremely difficult to address with PIC simulations because it typically requires observation of long-path-length evolutions with both high resolution and statistics.

5. Conclusions

PIC simulations have been employed to show that beams with high space-charge intensity transported in linear applied focusing channels can withstand large initial density-profile nonuniformities without suffering excessive emittance growth or loss of beam control as the beam evolves to a more uniform density-profile via collective processes. Simple theoretical models based on system conservation constraints have been used to parametrically bound the expected emittance growth and further support the conjecture that a wide range of perturbations can be tolerated [3,4]. This has important implications in the operation of practical machines because it shows that many processes leading to density nonuniformities can be tolerated in space-charge-dominated beams.

Continuations of these studies are examining the combined role of beam envelope mismatch in collective relaxation processes and modifications induced by alternating-gradient (periodic) focusing. Extensions of the theory already completed find little modification to results presented here when the energy associated with rms beam mismatch is transferred from the initial to the final state [4]. Preliminary simulation results also indicate that even though system energy is not conserved for alternating gradient focused beams, the continuous focusing theory based on system energy conservation provides reasonable emittance growth estimates if the beam maintains rms matched conditions. This follows because after an initial transient evolution, the regular focusing cycle of a periodic lattice should not pump or remove net energy from a stable beam core with uniform density and a matched envelope. Alternating gradient focusing also adds considerable richness to the spectrum of collective modes supported and launched, which further enhance phase mixing and nonlinear collective interactions smoothing the beam profile.

References

[1] S.S. Yu, S. Eylon, E. Henestrosza, D.P. Grote, Space charge dominated heavy ion beams in electrostatic quadrupole (esq) accelerators, in: Proceedings of the Workshop on Space Charge Dominated Beams and Applications of High Brightness Beams, Bloomington IN, 1995, p. 134.

[2] S.M. Lund, R.C. Davidson, Phys. Plasmas 5 (1998) 3028.

[3] S.M. Lund, J.J. Barnard, E.P. Lee, Emittance growth from the thermalization of space-charge nonuniformities, in: Proceedings of the XX International Linac Conference, Monterey, CA, 2000, Stanford Linear Accelerator Center, SLAC-R-561, Stanford, CA, 2001, p. 290 and MOE11.

[4] S.M. Lund, J.J. Barnard, E.P. Lee, R.C. Davidson, Beam emittance growth from the collective relaxation of space-charge nonuniformities: Part i—Theory, submitted for publication.

[5] M. Reiser, Theory and Design of Charged Particle Beams, Wiley Inc., New York, 1994.

[6] R.C. Davidson, Physics of Nonneutral Plasmas, Addison-Wesley, Reading, MA, 1990, re-released, World Scientific, Singapore, 2001.

[7] T. Wangler, K. Crandall, R. Mills, M. Reiser, IEEE Trans. Nucl. Sci. NS-32 (1985) 2196.

[8] D.P. Grote, A. Friedman, I. Haber, W. Fawley, J.-L. Vay, Nuc. Instr. and Meth. A 415 (1998) 428.

[9] S.M. Lund, J.J. Barnard, J. Miller, On the relaxation of semi-Gaussian and k–v beams to thermal equilibrium, in: Proceedings of the 1995 Particle Accelerator Conference, Dallas, TX, IEEE Piscataway, NJ 08855, 1995, p. 3278.

[10] P.M. Lapostolle, IEEE Trans. Nucl. Sci. NS-18 (1971) 1101.